Combustible Gases and Early Fire Detection: an Autonomous System for Wireless Sensor Networks

A. Somov[†], D. Spirjakin[♣], M. Ivanov[♣], I. Khromushin[♣], R. Passerone[†], A. Baranov[♣], and A. Savkin[♣]

[†]Dept. of Inf. Engineering and Computer Science
University of Trento
{somov, roby}@disi.unitn.it

[♣]Dept. of High Tech Radio-Electronics
Moscow State Aviation Technological University
radio@mati.ru

ABSTRACT

Fires or toxic gas leakages may have grave consequences like significant pecuniary loss or even lead to human victims. In this paper we present an autonomous wireless sensor system for early fire and gas leak detection. The system consists of two modules: a gas sensor module and a power management module. The operation of the gas sensor module is based on the pyrolysis product detection which makes it possible to detect fire before inflammation. In addition, the on board gas sensor can identify the type of leaking gas. A generic energy scavenging module, able to handle both alternating current and direct current based ambient energy sources, provides the power supply for the gas sensor module. The harvested energy is stored in two energy buffers of different kind, and is delivered to the sensor node in accordance to an efficient energy supply switching algorithm. At the end of the paper we demonstrate the experimental results on gas detection, energy consumption evaluation, and show how to ensure the system autonomous operation.

Categories and Subject Descriptors

C.3 [**Special-Purpose and Application-Based Systems**]: Real-time and embedded systems

General Terms

Design, Performance, Experimentation, Management, Measurement.

Keywords

Sensor node, energy efficiency, gas sensor, energy scavenging, power management.

1. INTRODUCTION

Efficient environmental monitoring with sensor networks covering large territories and ensuring continuous monitoring of wildfires and toxic gases can be regarded as a problem of top priority [2]. From a technical point of view, the wild land fire problem, for instance, has not been solved yet [3].

Though satellites are able to provide wide area sensing, in terms of real-time spatial resolution and sensitivity, this method has considerable restraints. Moreover, it is associated with the exceptionally high deployment and operational costs, which remains the factor of decisive importance [14, 27].

Another well-known approach to monitoring wild fires or gases leakage is based on getting data on the emissions source. With the ultrasensitive instrumentation aboard the vehicles (airplanes, trailers, etc.), it is possible to acquire data in cross patterns [3]. Apart from the fact that this method requires operation and maintenance personnel to be involved in, spatial and time resolution is limited to a point measurement at the vehicle current location. On top of that, sensitivity in the case of airborne platforms should be extremely high so as to secure the high-altitude detection of ground emissions after the gases have propagated to a considerable distance from the sources.

During the last few years, the paradigm of Wireless Sensor Networks (WSN) [1] has been adopted to tackle this problem. Cheap and tiny wireless sensor devices which operate in a cooperative and autonomous manner deployed over a territory may detect hazardous gases and monitor wild fires [4]. There are two main strategies used by sensor nodes to detect a wild fire. The first strategy is based mostly on temperature, relative humidity and barometric pressure sensors [2, 5], whereas the second uses smoke detectors [6]. The systems of these kind described in [2, 4, 5], however, can only detect the direct flame. The system referred to in [5], for instance, is intended for detecting and localizing a small fire (about tens of square meters). This means that in most cases the sensor nodes with the capabilities of direct fire detection are not useful. For instance, the authors of [2] managed to record the flame passage in California, USA, using the WSN facilities, but the sensor nodes were rapidly destroyed and the fire was extinguished only at the final stage. Thus, the primary goal of sensor nodes is to detect fire at an early stage [6].

The high power consumption of combustible gas detection and fire monitoring systems [7, 24, 25, 26] is also a limiting factor for nodes deployment. The sensor nodes used for this specific application with on-board batteries can not really last for a long time. So, the second goal is to prolong the long-term operation of the sensor nodes.

To overcome the lifetime problem, various research labs and commercial companies have developed sensor platforms [15-22] with energy scavenging technology [8], which collect energy from the environment. For instance, there are platforms that harvest

energy from ambient vibration [18, 22], solar radiation [16, 17, 20, 21], and wind energy [19]. However, these platforms either have an already integrated harvesting component (which makes them inflexible) [15-18, 20, 21] or contain a single energy buffer [15, 18, 20-22] to save energy for later use. Typical energy buffers are, however, unreliable: super capacitors have significant leakage current, while rechargeable batteries have a limited number of useful charge-discharge cycles [16], limiting the advantages of the scavenging technology.

In this paper we present a fully *autonomous* system for *fire detection* and *gas leak detection*. The system contains two modules: the gas sensor module and energy scavenging module. The developed gas sensor module allows the fire and gas leaks to be detected before the inflammation and smoke formation (on the basis of the pyrolysis product detection). To support an energy efficient operation of the gas sensor node we investigated various modes of heating the sensor and analyzed the dependence of its sensitivity on the temperature of the sensitive layer. In addition, the designed energy scavenging module (ESM) supports the long term operation of the entire system. This module enables efficient ambient energy collection, conversion, storage, and usage. The experimental results on gas detection as well as measures on tests conducted on the ESM are presented.

The paper is organized as follows: Section 2 will overview the developed system, present the system architecture. Section 3 will introduce the reader to the hardware implementation of the system. Experimental results on the sensitivity investigation, efficient energy consumption, and experimental system deployment are presented in Section 4. Finally, we conclude and discuss our future work.

2. SYSTEM OVERVIEW AND PRINCIPLES OF OPERATION

The system consists of two modules: the gas sensor module and the energy scavenging module (ESM). Gas detection is performed by the gas sensor module, whereas the ESM is exploited as a power supply for it.

The main purpose of the designed gas sensor module is to allow one to get information about possible inflammation *prior to* the formation of smoke and the appearance of a direct flame [9], or to register the presence of a dangerous gas in the atmosphere (see Figure 1).

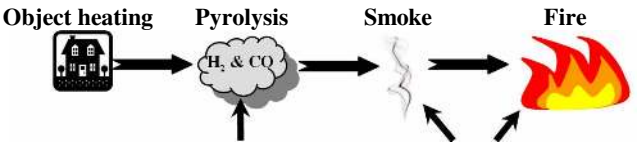

Our platform	Existent platforms
- pyrolysis;	- temperature, humidity [2, 5];
- combustible	- smoke [6];
gases.	- direct flame [2, 4, 5].

Figure 1. Fire formation and its detection.

We use a *temperature scanning procedure* of the sensing element of pre-fire (gas) detector to separate in time the processes which occur in the semiconductor layer's electronic subsystem from the relatively slow chemical processes which run on the catalytically active surface of the catalyst. This process increases the sensors' sensitivity and selectivity. The working principle of the pre-fire sensor operation is based upon the detection of pyrolysis products due to smoldering or overheating of combustible and electric insulating materials, primarily carbon oxide (CO) and hydrogen (H_2).

The goal of the ESM is to mediate between an energy harvesting component and the gas sensor module, providing a flexible modular system, and to increase the gas sensor module lifetime. This module supports various energy scavenging technologies [8].

Figure 2 shows the hardware architecture of the developed system. The semiconductor sensor acts as a sensing element to determine the gas composition of the environment. The data-conversion line (sensor – operational amplifier – microcontroller) converts the gas-composition dependent parameters of the sensor to digital format/code. A microcontroller-based drive/control circuit sets the required operation modes of the node, implements the mechanism for obtaining the digital code from the analog-to-digital conversion line, and provides preliminary data processing and compilation for the data wireless transmission module circuit.

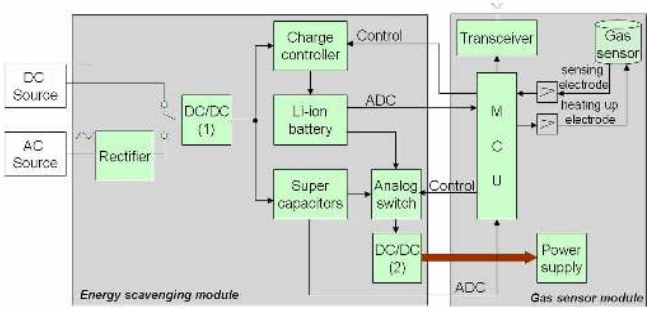

Figure 2. Architecture of autonomous gas detection system.

The ESM architecture contains seven main blocks. The first block DC/DC(1) operates as a transformer. It is supplied either by the "AC-based" ambient source (i.e., noise, vibrations) through the Rectifier, or by the "DC-based" ambient source (i.e., solar radiation, thermal energy). The purpose of the DC/DC(1) block is to provide the ESM with a stable input voltage. Super capacitors, wired in series with each other and in parallel with the DC/DC(1) block, operate as a buffer. In other words, if the ambient source is available the system exploits environmental energy transformed to the necessary voltage level by the DC/DC(1) block. Otherwise, the system can be supplied by the super capacitors in case they are charged. The sensor node monitors the voltage level available in the super capacitors to verify if they can be a power supply for the system or not. The third power supply depicted in the system architecture is a Li-ion battery. The Li-ion battery is a backup power supply. The charging/discharging state of the battery is controlled by the Charge Controller which, in turn, is managed by the sensor node. Thus, the ESM is designed in such a way that a sensor node can be supplied by one of three energy sources: super capacitors, Li-ion battery or directly by the environmental energy source. However, a user must specify the type of ambient source (both AC-based and DC-based harvesting components are supported, although the two cannot be present at the same time) using "jumpers" before the sensor network deployment. Before the DC/DC(2) block generates the required output voltage to

supply the sensor node, the Analog switch chooses the power supply on the basis of the voltage level available and power management algorithm described in the next paragraph. The Analog Switch and the Charge Controller are managed by the onboard sensor node microcontroller.

The power management algorithm was designed in order to increase the lifetime characteristics of the system. The algorithm is developed in accordance with the hardware components lifetime cycles and the availability of the necessary voltage level to supply the sensor node. The system adopts the following energy strategy:

- take what is available;
- use economically;
- use efficient conversion and optimal power harvesting for high-quality performance.

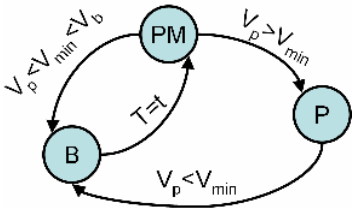

Figure 3. FSM explaining the choice of power supply for a gas sensor node.

The Finite State Machine (FSM) depicted in Figure 3 explains how the ESM handles the power sources to increase the long term operation of the entire network. Since the Li-ion battery has the shortest lifetime, which mostly depends on the number of charge-discharge cycles, its energy is the most valuable. The environmental power supply is inexhaustible, but unstable. Thus, a Power Management (*PM*) algorithm at first considers the ambient power source and super capacitors as a primary power supply *P*. The battery is defined as a backup or secondary power supply *B*. Initially, *PM* compares the available voltage level of the primary power source V_p with the minimal voltage threshold V_{min} needed to supply the load. If $V_p \geq V_{min}$, *PM* selects *P* as a power supply for the load. In case the *P* source becomes unavailable, the load is switched to the backup *B*. The algorithm then monitors the level V_p every *T* time units, and switches back to *P* when environmental energy is available again. Otherwise, *B* remains as a power supply for the load.

3. HARDWARE DESIGN

In this section we describe both modules implementation in details and discuss the choice of components.

3.1 Gas Sensor Module Implementation

The gas sensor module is shown in Figure 4. The main unit of the gas sensor module is a Microcontroller Unit (MCU). For the designed node we have chosen the 8-bit MCU ADuC836. It has low power consumption, power supply monitor (both features are important for energy constrained WSNs), two analog-to-digital converters, enough Flash/EE memory and an on-chip debug system.

The MCU communicates with the gas sensor through two OPA2340 operational amplifiers, optimized for low voltage operation. One amplifier is connected to the sensing electrode of the sensor whereas the second one is connected to the heating up electrode. Typically, a gas sensor is the main energy sink in an autonomous embedded system. To overcome this problem, our gas sensor module uses a pulse mode of gas measurement. Pulse Width Modulation (PWM) signals with a ~1 kHz frequency and 3.3 V amplitude go from the MCU control circuit to the sensor's heating unit with a 30-second interval. As a result, the sensing element warms up. If there are flammable, toxic, or explosive gases of various compositions and concentrations in the atmosphere, the conductivity of the semiconductor sensor's sensitive layer changes. By adopting this mode, it was possible to reduce the total power consumption of the gas sensor from more than 100 mW (typical of continuous operation mode [10]) to the level of 30 mW, thereby enabling the long-time battery supply of the sensor. Semiconductor and thermo-catalytic sensors made using aluminum-oxide membranes [11, 12] are a perfect fit for the pulse mode of measurement.

Figure 4. Gas sensor module.

The measured data (i.e., the presence of gas, its composition and concentration) converted by the Analog-to-Digital Converter (ADC) to a digit serial code go to the MCU control circuit where they are preprocessed. The resulting data is passed to the wireless transmission module TG-ETRX2, a ZigBee standard [29] module using the 2.4 GHz frequency channel.

3.2 Energy Scavenging Module Implementation

The implemented four-layer 50x70 mm prototyping board of the ESM is shown in Figure 5. The ESM supports a 5.5 W ambient power source (max input current = 500 mA; max voltage = 11 V), and a "jumper" is used to switch between the AC and DC source. The AC-to-DC voltage conversion is performed by a standard DB102S diode rectifier and an electrolytic capacitor. Further stabilization of the DC voltage to 4.5 V is implemented by MAX1672, a step-up/down DC/DC converter.

Two super capacitors wired in series to reduce leakage current are used as the primary energy buffer. In line with [16], we have chosen Cooper Bussmann's 2.5 V, 22 F capacitors as a trade-off in terms of capacitance and leakage current. The series wiring of super capacitors requires balancing to guarantee equal voltage sharing. We applied passive balancing to maintain similar

voltages between the super capacitors where the leakage currents may be slightly different. Passive balancing uses equal value resistors in parallel with the super capacitors to let a small current flow (of the order of 2-3 µA that does not essentially affect the sensor node lifetime) between the super capacitors, thus keeping the voltages at the same level.

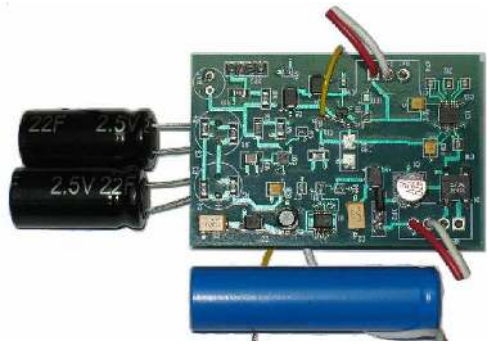

Figure 5. Energy scavenging module.

The secondary energy buffer's functions are performed by a EEMB LIR17650 Li-ion rechargeable battery having 3.7 nominal voltage and 1400 mAh typical capacity. Having no memory effect, lithium rechargeable batteries provide a high number of charge-discharge cycles (in comparison to NiMH batteries), highest density and lowest leakage [16]. However, they require a more complex charging circuit, e.g., a special charge controller. The MIC79110 battery charge controller is used to charge the secondary energy buffer. This integrated circuit performs a number of functions needed for thorough battery maintenance, i.e., thermal shutdown, current limit and reverse current protection, and precise voltage control. The secondary buffer is charged by the primary buffer. However, with the primary buffer being charged and the ambient power source providing stable voltage, the secondary buffer can be charged directly. The Single Pole Double Throw (SPDT) switch MAX4624 having high current carrying capability and low power consumption is used to choose between the primary and secondary power buffer to supply the wireless sensor node. The ESM's output voltage of 5 V is provided using another MAX1672 step-up/down DC/DC converter which provides voltage stabilization. In order to ensure interconnection between the ESM and the gas sensor module, we have used a 4-pin connector for charge/monitor battery control, super capacitor voltage monitoring and analog switch control.

4. EXPERIMENTAL RESULTS

In this section we present the experimental results on gases detection and sensitivity of the system. We also investigate energy consumption at various heating profiles of the sensor, evaluate the ESM, and discuss our experimental system deployment.

4.1 Pre-fire Detector Response

The pre-fire detector response experiment describes how the sensor node sets the pre-fire detector in operating mode. In addition, we show the difference in time response between a bulk-substrate sensor [13] and the sensor (used in this work) made using an aluminum-oxide membrane [11].

Figure 6a shows the oscilloscope display of the voltage pulses heating the sensor's sensitive layer. The pulse frequency is 675 Hz which ensures effective control of the sensor temperature making feedback possible. The heating time depends on the preset temperature, the heating pulse duration and the sensor design.

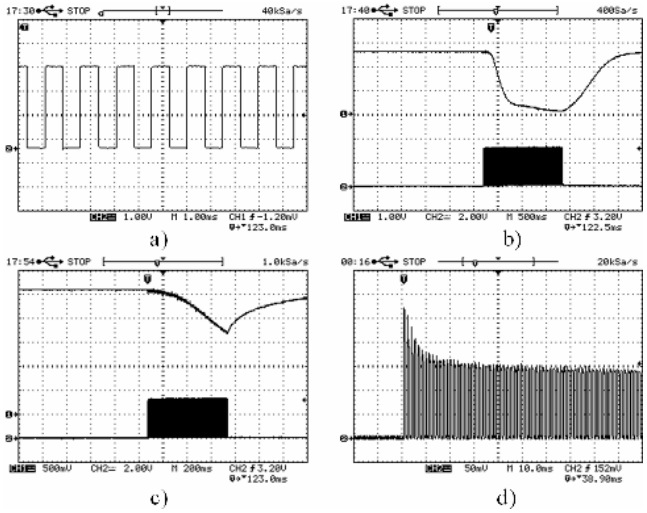

Figure 6. (a) 50% PWM generated by microcontroller, (b) variation in the sensitive layer's resistance of the bulk-substrate sensor in relative units (upper graph) and PWM generated by microcontroller (lower graph), (c) variation in the sensitive layer's resistance (in relative units) of the sensor made using the aluminum-oxide membrane (upper graph) and PWM generated by microcontroller (lower graph), and (d) variation in current running through the sensor's (the sensor made using the aluminum-oxide membrane) heating element.

For a semiconductor sensor made on an aluminum-oxide membrane using micromachining technology (Figure 6c), the Pulse Width Modulation (PWM) time for a 450 ^{o}C operating temperature of the sensor is of the order of 500 ms (cf. 1.5 s for a bulk-substrate sensor, Figure 6b). Control of PWM pulse duration ensures various heating/cooling profiles including gradual (smooth) heating of the sensor.

4.2 Gases Detection

Figure 7 shows the sensor's response in the absence and presence of methane (0.2 % CH_4), alcohol fume and wood pyrolysis.

After analyzing the obtained results, one can see that, in the absence of toxic and inflammable gases, variation in temperature of the semiconductor sensitive layer (the sensor is ON) leads to an increase of its conductivity and, respectively, a drop of its voltage. After the heating pulse termination (the sensor is OFF), the layer's conductivity goes back to the initial value (Figure 7, curve 1).

Wood pyrolysis is accompanied by H_2 and CO emission in the atmosphere. With their liberation, after termination of the heating pulse, the sensitive layer's conductivity rapidly drops at the first stage. However, after a considerably longer time, it steps up to the initial level (Figure 7, curve 2).

If the sensitive layer interacts with methane (as it can be seen from Figure 7, curve 3), a noticeable drop in the sensitive layer's conductivity will occur, while its recovery will take several seconds. In the case of alcohol fume measurement, we have the experimental relationship of the 3rd type. The sensitive layer's

conductivity remains practically unchanged, but getting back to initial conductivity after heating termination requires maximum time.

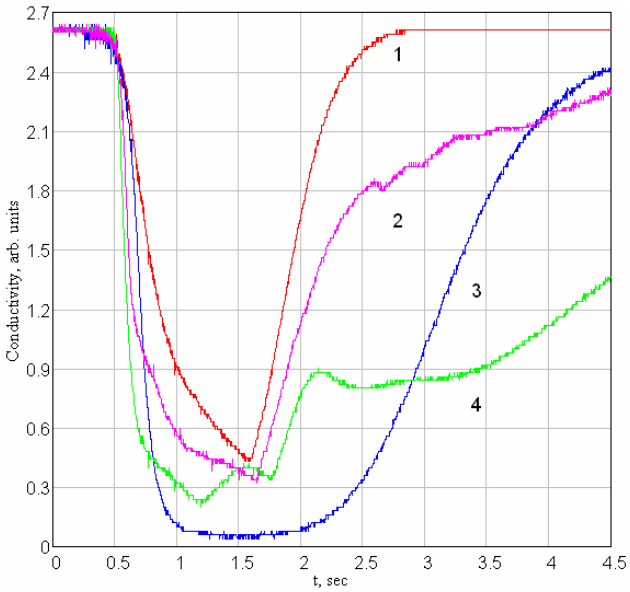

Figure 7. Sensor's response to various gases at T = 500 °C: (1) – the air; (2) – pyrolysis; (3) – 0.2 % CH_4; (4) – alcohol fume.

One may conclude from the above that, provided the sensitive layer's conductivity is measured within 0.2-0.5 s after heating termination, it is possible to separate mixed gases and define gas types and concentrations.

4.3 Sensitivity Investigation

Sensitivity plays significant role in reliability of fire and gas detection. At the same time, sensitivity impacts on the system energy consumption: the more the sensor is heated up, the more sensitive it is, hence more energy it requires. In this section we investigate sensitivity of the sensor in terms of temperature (PWM of heating pulses) and figure out if heating with high temperature is really essential.

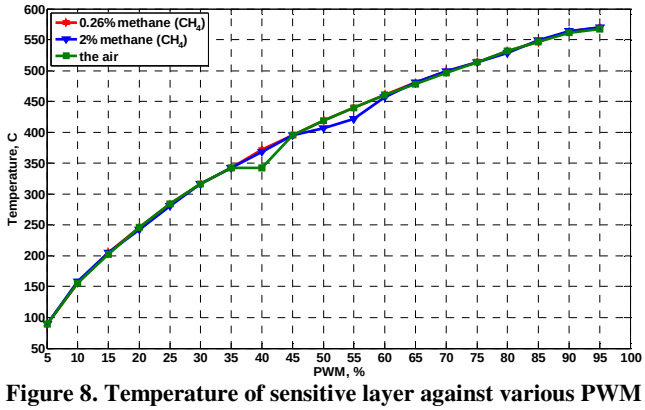

Figure 8. Temperature of sensitive layer against various PWM modes under normal conditions.

Figure 8 shows how the temperature of sensor`s sensitive layer depends on various heating modes. It is not recommended to heat the sensor to higher then 550 ^oC since the sensor can be damaged at 600 ^oC. This graph shows that heating the sensor with a PWM of more than 85 % is dangerous.

Figure 9 presents how the sensor response to gases depends on PWM heating modes. The higher is the temperature of the sensitive layer and the higher the concentration of the combustible gas (methane), the better the response. Based on the magnitudes of these curves we graphed Figure 10.

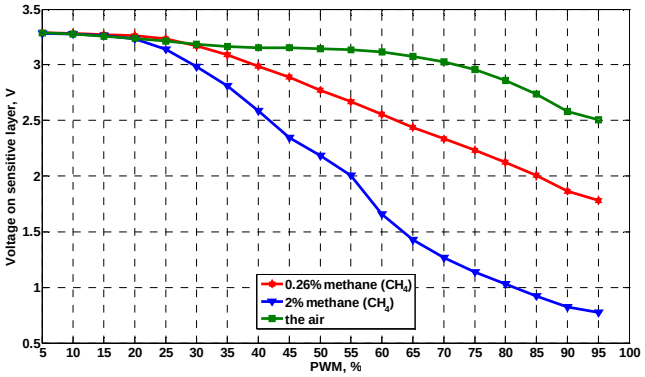

Figure 9. Sensor response against various PWM heating modes.

Figure 10 represents the sensor sensitivity. Zero sensitivity corresponds to sensor response to the air at appointed temperature. The graph shows that the optimal sensitivity is reached at the 75-80 % PWM.

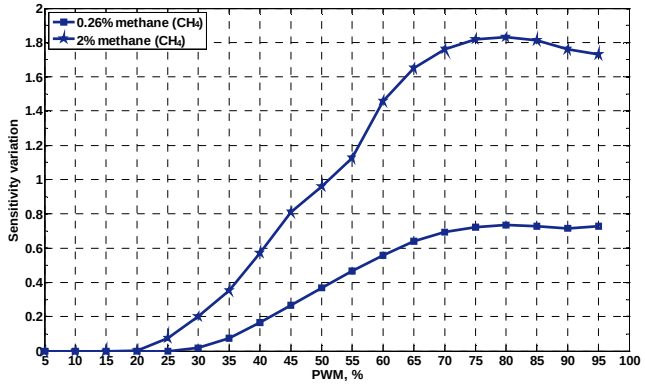

Figure 10. Sensitivity of the sensor.

The next section will investigate how various modes of PWM affect on energy consumption, so that we could determine the most energy efficient and reliable in terms of sensitivity heating profile of the sensor.

4.4 Energy Consumption

The main power sink in the system is the gas sensor. Much energy is being spent during its heating. That is why it is important to investigate energy consumption of the gas sensor.

Pulse Width Modulation (PWM) is a technique for electrical power control between fully *on* and fully *off* states. Obviously, to heat the sensing element up to a predefined temperature applying

Table 1. Gas sensor module energy consumption during the sensor heating.

PWM, %	For 450 °C			For 550 °C		
	Heating time, s	Energy consumption, mJ	Gain in energy as against 100%, %	Heating time, s	Energy consumption, mJ	Gain in energy as against 100%, %
20	2.1	251	-100	5	576	-150
30	0.91	163	-30	2.5	432	-87.5
40	0.6	143	-14.3	1.2	277	-20
50	0.43	128	-2.4	0.8	230	0
60	0.33	118	5.7	0.62	214	7
70	0.26	109	13.3	0.5	202	12.5
80	0.24	115	8.6	0.45	207	10
100	0.21	125	0	0.4	230	0

various duty cycles will take various ranges of time, and hence consume various levels of energy. In this section we will demonstrate how a user may perform an efficient power management of the gas sensor node using various heating profiles for the sensor.

The sensor resistance is a function of temperature [28] and can be computed as:

$$R = R_0 \cdot (1 + \alpha \cdot (T - 20°\text{C})) \quad (1)$$

where R_0 is the resistance of the heating layer of the semiconductor sensor (12 Ohm) under normal conditions, α is the temperature coefficient of resistance (0,0027 ^{1}/°C in our case), T is the temperature (in °C). The resistance of the sensor at 450 °C (R_{450}) and 550 °C (R_{550}) is 25.9 Ohm and 29.1 Ohm respectively. Because the resistance increases with temperature, the current decreases when the sensor is heated up (see Figure 8d). The initial current can be calculated using Ohm's law:

$$I_{start} = \frac{U}{R} = 275mA \quad (2)$$

where U is a voltage during heating (3.3 V in our case). The currents $I_{end\ 450}$ and $I_{end\ 550}$ at R_{450} and R_{550} are 127 mA and 113 mA respectively.

Next, using the *trapezoidal rule* and knowing empirically the time required for the sensor heating (see Table 1) till its "on-position" we calculated the magnitude of the charge q_{450} necessary to heat the sensor up using a constant current: 38 mA·s. Hence, energy consumption during the constant sensor heating up till 450 °C can be calculated as:

$$E_{450} = q_{450} \cdot U = 125mJ \quad (3)$$

However, to calculate the energy consumption under the same conditions, but using another duty cycle, 80 % for instance, we cannot simply multiply E_{450} by 0.8. In fact, empirically, we established that the heating up time for sensors at various duty cycles does not change linearly.

Table 1 shows the energy consumption of the gas sensor module at the time of sensor heating and represents how the heating time of the sensor depends on the duty cycle of the heating pulses. According to our experiments, a 70 % duty cycle is the most efficient for both 450 °C and 550 °C heating profiles. Negative numbers in the "Gain in energy" column of Table 1 relate to long term of heating. For low duty cycles, the heating layer cools down enough, so that next heating pulse must heat it up till the previous level and heat it up to the next level as well. Based on data presented in Table 1 the system may be adjusted by the user in accordance with application requirements.

4.5 Energy Scavenging Module Evaluation

To evaluate the ESM, we conducted three experiments to: (a) charge the super capacitors from a DC-source, i.e., solar panel BP SX305M, and then charge the battery using the same source, (b) charge the super capacitors from an AC-source, and (c) discharge both the battery and the super capacitors by connecting the gas sensor module.

The solar panel was installed indoors in the electronic lab with bright internal illumination. Then we connected the solar panel wires to the ESM power connector. The multimeter was connected directly to the pins of the super capacitors taking into consideration that they are wired in series. The "jumper" was installed in *DC ambient source* position.

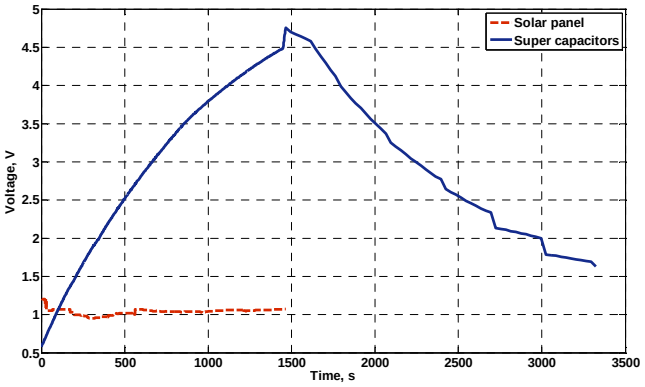

Figure 11. The charging and discharging of super capacitors.

Figure 11 shows the voltage generated by the solar panel during the experiment. The purpose of this experiment is to demonstrate that the super capacitors could be promptly charged from the ambient source, and that they are able to support an uninterrupted operation of the gas sensor module in real conditions. The voltage was stable at approximately 1.1 V. Two super capacitors were fully charged in 1464 seconds (~25 minutes). Outdoor experiment

showed that in case of cloudy sky the charging of super capacitors takes 47 minutes.

Next, we connected the gas sensor module to the ESM. The gas module was programmed to scan ambient atmosphere and send the measured data once every five minutes. Because of the load, the super capacitors started discharging and reached the 1.6 voltage level (the module reset happened) in 1863 seconds (~31 minutes). Starting from this voltage level the ESM can not provide 5 V for the proper operation of the sensor module. Using the sleep mode of the MCU and the modem increases the module lifetime to 4290 seconds (~72 minutes).

To discharge the Li-ion battery (Figure 12) we connected the gas sensor module to the ESM and run the application of ambient atmosphere sensing and transmission of measured data once per ten seconds. Over a period of time equal to 176 minutes the battery was discharged from 4.18 V to 2.8 V. The graph shown in Figure 6 shows also the charging behavior of the Li-ion battery when supplied by the solar panel. It took 334 minutes to fully charge the battery (750 mAh) from 2.8 V to its maximum voltage (4.2 V).

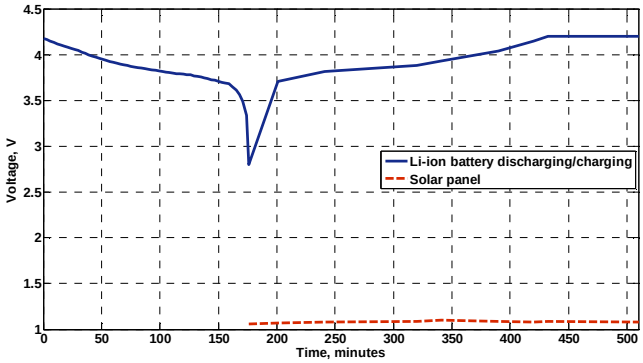

Figure 12. The charging of Li-ion battery with solar panel.

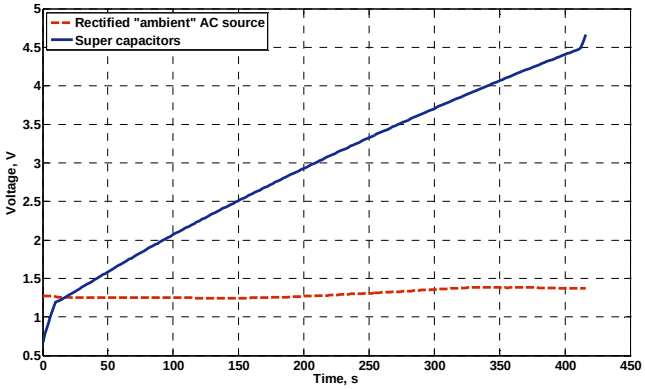

Figure 13. The charging of super capacitors with AC source.

Next, we discharged the super capacitors and began to charge them through the AC voltage generator (Figure 13). Since we did not have a harvesting component for noise or vibration capture, we carried out the experiment having simulated noise with the triple power supply HAMEG HM8040 and function generator HM8030. A digital multimeter Agilent 34411A measured with a 2 second sampling period the voltage level of the two super capacitors wired in series and recorded the data in a log-file. Obviously, the AC generator can not simulate an AC-based harvesting component exactly. However, the main purpose of this experiment was to verify the AC voltage rectifier made of a diode rectifier and an electrolytic capacitor.

The results are shown in Figure 13. Following [23], we simulated a piezoelectric converter which generates 3.5 V at 120 Hz. The goal of this experiment is to ensure that the ESM voltage rectifier can convert AC "ambient" voltage into DC voltage properly. We measured the rectified AC voltage and the voltage level of the super capacitors. The super capacitors were fully charged in 416 s (~7 minutes).

4.6 System Deployment

Having carried out the experiments on sensor's response, sensitivity, and energy consumption evaluation it was essential to prove the system autonomy.

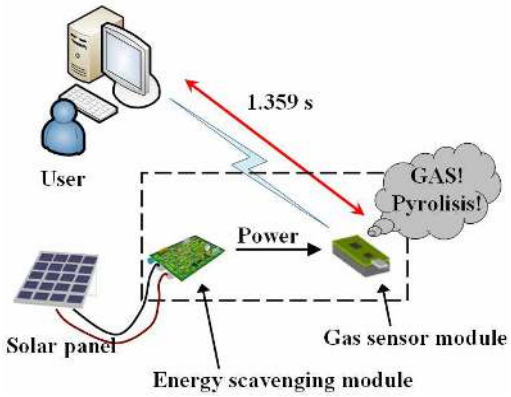

Figure 14. Schematic representation of the experimental deployment.

The autonomous wireless sensor system for combustible gases detection and wild fire monitoring was deployed in the campus of Moscow Aviation Technological University in October, 2009. The experimental setup is depicted in Figure 14 and includes the gas sensor module, the energy scavenging module, solar panel BP SX305M, laptop (since then called "host") to control the gas detection system, a methane-cylinder and piece of wood with a lighter to emulate the gas leakage or pyrolysis.

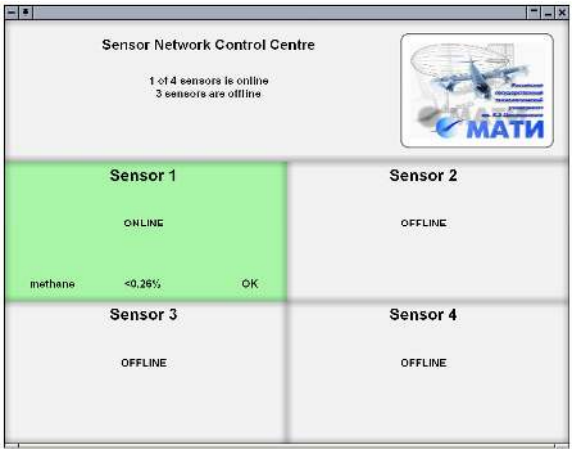

Figure 15. Interface for network control.

Between the system and the host (distance 15 meters) was organized a wireless network using the ZigBee standard [29]. A specifically designed "friendly" software interface shown in Figure 15 aims to facilitate the network management control. The screenshot shows that one sensor node, i.e., our system, was able to connect to the host. If the gas concentration is less than 2 %, and, in this case, is equal to 0.26 %, the "Sensor 1" window will be green. "OK" means that the system has enough energy for further operation. In case a gas concentration exceeds the 2 % threshold, the window will turn red and an alarm will go off.

Every 30 minutes we emulated either methane leakage or generated pyrolysis by setting the piece of wood on fire. The system measured the atmosphere and transmitted data to the host each 15 minutes.

We applied 450 °C, 70 % duty cycle of heating pulses profile. From 8 a.m. to 8 p.m. we monitored the voltage level on the super capacitors and the rechargeable battery of the energy scavenging module, and tracked the voltage generated by the solar panel. The three graphs shown in Figure 16 represent the voltage state during the 12-hour period.

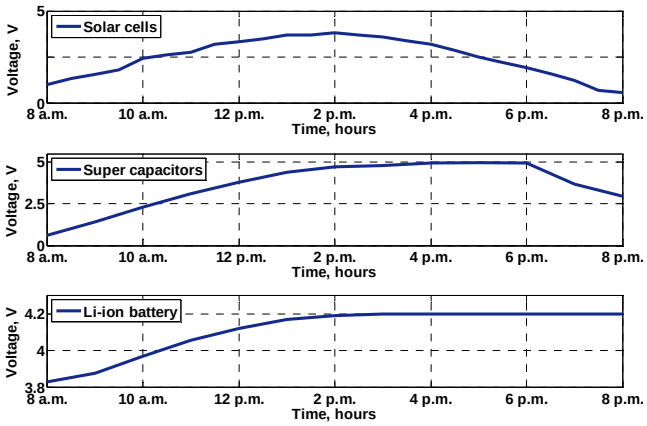

Figure 16. Voltage level on solar panel, super capacitors, and li-ion battery during 12-hour period.

At the time of the experiment it was a cloudless and sunny day. The battery was discharged from 4.2 V to 3.88 V (discharge cut-off voltage is 2.75 V) during the night. The super capacitors started to charge from the solar panel before 8 a.m. as it is depicted in the graph. Because the solar radiation is not strong in the morning, the battery had to be replenished, and because the system was operating – the caps were charging slowly. However, at around 4 p.m. they were fully charged (whereas the battery was fully charged at around 3 p.m.), so that the system had a chance to be supplied directly from the solar panel. Starting from 6 p.m. the solar panel could not generate enough energy to support the operation from the ambient source that led to a smooth super capacitors discharge. At the end of our experiment the battery was still fully charged. We should note that there is a lack of strong solar radiation in Russia during autumn, but it was sufficient for the stable system operation.

After that, we also determined the time spent for data inquiry (the last measured state of atmosphere) from the system. The host received the response from the gas sensor module in 1.359 seconds.

5. CONCLUSIONS AND FUTURE WORK

In this work we demonstrated a system for dangerous gases detection and early fire monitoring. An on-board gas sensor supports a pulse heating mode which promises significant energy savings. Also based on the physicochemical properties of the sensor we managed to devise an advanced algorithm for early fire detection. According to this algorithm, we can detect fire before its inflammation and even smoke formation proceed from pyrolysis product detection in the atmosphere.

Besides, we found a trade-off between sensitivity of the sensor and power consumption during its heating. The most energy efficient and reliable mode of system operation is at 70-80 % PWM, 450 °C heating profile. Experimental system deployment ensures its self-sufficiency.

Our future work aims at WSN deployment in real conditions and analysis of its operation. In order to decrease the system power consumption we are planning to use the gas sensors fabricated using advanced technologies for low power applications.

6. ACKNOWLEDGMENTS

We would like to thank Dr. A. Pisliakov and Dr. A. Vasiliev for providing the sensors [12], [13] for prototype development and for conducting experiments. This work was sponsored in part by the Berkeley Wireless Research Center, USA, and by a grant from Fondazione Caritro.

7. REFERENCES

[1] C.-Y. Chong, S. P. Kumar, "Sensor networks: Evolution, opportunities, and challenges," Proceedings of the IEEE, vol. 91, no. 8, pp. 1247-1256, August 2003.

[2] D. M. Doolin, N. Sitar, "Wireless sensors for wildfire monitoring," Proceedings of Sensors and Smart Structures Technologies for Civil, Mechanical, and Aerospace Systems Conference, vol. 5765, San Diego CA, USA, 7-10 March, 2005.

[3] A. Volokitina, M. Sofronov, and T. Sofronova, "Topical scientific and practical issues of wildland fire problem," Mitigation and Adaptation Strategies for Global Change journal (Springer Netherlands), vol. 13, no. 7, pp. 661-674, August 2008.

[4] T. Antoine-Santoni, J. F. Santucci, E. De Gentili, B. Costa. "Wildfire impact on deterministic deployment of a wireless sensor network by a discrete event simulation," 14th IEEE Mediterranean Electrotechnical Conference, pp. 204-209, 5-7 May, Ajaccio, France, 2008.

[5] Y. Li, Z. Wang, Y. Song, "Wireless sensor network design for wildfire monitoring," 6th World Congress on Intelligent Control and Automation, pp. 109-113, Dalian, China, 2006.

[6] Z. Chaczko, F. Ahmad, "Wireless sensor network based system for fire endangered areas," 3rd International Conference on Information Technology and Applications, vol. 2, pp. 203-207, Australia, July, 2005.

[7] S. Nakano, K. Yokosawa, Y. Goto, K. Tsukada, "Hydrogen gas detection system prototype with wireless sensor networks," IEEE Sensors, pp. 159-162, USA, October, 2005.

[8] S. Roundy, P. K. Wright, J. M. Rabaey, Energy Scavenging for Wireless Sensor Networks. Kluwer Academic Publishers Group, 2003.

[9] A. A. Vasiliev, V. I. Filipov, I. M. Olikhov, et al., "Gas sensors for the detection of pyrolysis of combustible gases," 8th International Meeting on Chemical Sensors, Switzerland, 2000.

[10] [Online] http://www.figarosensor.com/products/2610pdf.pdf, February, 2009.

[11] A. A. Vasiliev, R. G. Pavelko, S. Yu. Gogish-Klushin et al., "Alumina MEMS platform for impulse semiconductor and IR optic gas sensors," Sensors and Actuators B: Chemical, vol. 132, issue 1, May 2008, pp. 216-223.

[12] A. A. Vasiliev, S. Yu. Gogish-Klushin et al., "A novel approach to the micromachining sensors: the manufacturing of thin alumina membrane chips," Eurosensors XVI, Czech republic, 2002.

[13] V. V. Malyshev, A. V. Pislyakov, "Investigation of gas-sensitivity of sensor structures to carbon monoxide in a wide range of temperature, concentration and humidity of as medium," Sensors and Actuators B: Chemical, vol. 123, issue 1, April 2007, pp. 71-81.

[14] B. Leblon, "Monitoring forest fire danger with remote sensing," Natural Hazards journal, Publisher Springer Netherlands, vol. 35, no. 3, pp. 343-359, July 2005.

[15] Y. H. Chee, M. Koplow, M. Mark, et al., "PicoCube: A 1cm^3 sensor node powered by harvested energy", Design Automation Conference 2008, pp. 114-119, USA, 2008.

[16] X. Jiang, J. Polastre, and D. Culler, "Perpetual environmentally powered sensor networks", 4th Int. Symposium on Information Processing in Sensor Network, pp. 463-468, 2005.

[17] P. Dutta, J. Hui, J. Jeong, et al., "Trio: Enabling sustainable and scalable outdoor wireless sensor network deployments", 5th International Symposium on Information Processing in Sensor Network, pp. 407-415, 2006.

[18] R. N. Torah, M. J. Tudor, K. Patel, et al., "Autonomous low power microsystem powered by vibration energy harvesting", 6th annual IEEE Conference on Sensors, USA, 2007.

[19] C. Park and P. H. Chou, "AmbiMax: Autonomous energy harvesting platform for multi-supply wireless sensor nodes", 3rd Annual IEEE Communications Society on Sensor and Ad Hoc Communications and Networks, vol. 1, pp. 168-177, September, 2006.

[20] F. Simjee and P. H. Chou, "Everlast: Long-life, supercapacitor-operated wireles sensor node", International Symposium on Low Power Electronics and Design, pp. 197-202, 2006.

[21] V. Raghunathan, A. Kansal, J. Hsu, J. Friedman, M. Srivastava, "Design considerations for solar energy harvesting wireless embedded systems", 4th International Symposium on Information Processing in Sensor Networks, pp. 457-462, April, 2005.

[22] Perpetuum, www.perpetuum.co.uk, 2009.

[23] S. Roundy, P. Wright, J. Rabaey, "A study of low level vibrations as a power source for wireless sensor nodes", Computer Communications, vol. 26, issue 11, pp. 1131-1144, 2003.

[24] S. So and G. Wysocki, "Ultra efficient laser spectroscopic trace-gas sensors for sensor networks and portable chemical analysis," Innovation Forum 2009, Princeton school of engineering and applied science, May, 2009.

[25] JLM innovation, ZigSens platform, http://www.jlmi.de/products/zigsens, 2009.

[26] F. Linnarsson, P. Cheng, B. Oelmann, "SENTIO: A. Hardware Platform for Rapid Prototyping of Wireless Sensor Networks," IEEE The 32-nd Annual Conference of the IEEE Industrial Electronics Society 2006.

[27] R. Burgan, R. Klaver, and J. Klaver, "Fuel models and fire potential from satellite and surface observations," International Journal of Wildland Fire, 8 (3), pp. 159-170, 1998.

[28] H. Kuchling, "Handbook of physics" [Russian translation], Mir, Moscow, 1982, p.315.

[29] IEEE Computer Society, http://www.ieee.org, "802.15.4 Wireless Medium Acces Control and Physical Layer Specifications for Low-Rate Wireless Personal Area Networks," 2003.